Recovery of cobalt ions from diluted solutions by means of protonated dry alginate beads

Alvaro Aracena [1], Sebastián Padilla [1], Oscar Jerez [2]

[1] Escuela de Ingeniería Química, Pontificia Universidad Católica de Valparaíso, Avenida Brasil 2162, Cod. Postal 2362854, Valparaíso, Chile

[2] Instituto de Geología Económica Aplicada (GEA), Universidad de Concepción, Casilla 160-C, Concepción, Chile

Corresponding author: alvaro.aracena@pucv.cl (Alvaro Aracena)

Abstract: Mining effluents contain cobalt ions that can damage humans and flora. However, this metal also has high commercial value when recovered. The objective of this research work was to recover cobalt (Co^{2+}) from diluted solutions using a biosorbent, specifically protonated dry alginate beads (PDAB). Experimental work was carried out in batch from an initial concentration of 22×10^{-6} kg dm^{-3} Co^{2+} and 80 mg alginate. Variables such as agitation, pH solution, experimental time, isotherm values, and temperature were analyzed. Maximum cobalt recoveries were obtained at pH values above 5.0, reaching 60.6×10^{-3} kg kg^{-1} of PDAB. Cobalt recovery occurred with ion exchange mechanisms from alginate carboxyl group proton release. Experimental data had excellent fit with both the Lagergren kinetic model (pseudo-first order) and the Langmuir isotherm model. As temperature increased, cobalt recovery increased. The calculated activation energy was 12.8 kJ mol^{-1}. Compositional measurements obtained by scanning electron microscope and energy-dispersive X-ray spectroscopy for alginate cross-sections showed uniform distributions of cobalt concentrations throughout the spherical alginate structure, independent of solution pH, contact time, or temperature. Furthermore, elution gave significant cobalt re-extraction (98.2%) and demonstrated PDAB reusability.

Keywords: recovery mechanism, cobalt ions, alginate beads, kinetic adsorption model, elution

1. Introduction

Different heavy metals are released to water sources via liquid waste called effluent. One source of this discarded mixture of water and acid comes from the mining industry, which is known to possess significant amounts of heavy metals. Such effluents have increased over the years due to mineral processing and mining operations (Feng et al., 2000). The composition of these effluents usually contains copper, cobalt, zinc, cadmium, lead, etc. These metals are highly toxic, and thus generate negative impacts on flora, fauna, and humans. Of these metals, cobalt has a variety of complex effects manifesting as neurological, cardiovascular, and endocrine conditions (Leyssens et al., 2017). At the same time, from a commercial point of view, there has been growing interest in cobalt over recent years due to its effectiveness as a corrosion inhibitor in lead anodes via electrowinning. On the other hand, cobalt has recently been used in the lithium-ion battery manufacturing industry as CoO (Wang et al., 2002), gel-assisted synthesis (Huang et al., 2019); and for sodium-ion batteries (Qi et al., 2019; Jiang et al., 2019), among other uses of batteries. Based on this industrial application alone, effluent metal recovery is advisable.

There are a variety of methods for recovering cobalt in solution, such as precipitation in ammoniacal media (Güler and Seyrankaya, 2016), membrane separation (Sürücü et al., 2010), or solvent extraction (Hachemaoui and Belhamel, 2017). The main disadvantages of these methods are sludge generation and low efficiency due to very low concentrations of cobalt (<50 ppm), which makes recovery difficult. An alternative method for small concentrations of cobalt recovery is biosorption. Adsorption and ion

exchange processes are widely used for eliminating heavy metals from aqueous effluents and have competitive advantages like low cost, material reuse, etc. Thus ion exchange recovery mechanisms have broad study potential, especially biosorption with natural polymeric materials like alginate. This biosorbent can be manipulated to form beads of controlled size, good physical and chemical properties, as well as high porosity (Ibáñez and Umetsu, 2002). Alginate beads have already been demonstrated for use in recovery of chromium (Ibáñez and Umetsu, 2004), cadmium (Ibáñez and Umetsu, 2008), zinc (Ibáñez and Aracena, 2014), nickel (Aracena et al., 2015) and copper (Aracena et al., 2019), among other metals. This study delineates cobalt recovery through dilute solution extraction in order to reuse it through methods like precipitation.

The objective of this work was: to analyze cobalt ion recovery through the use of protonated dry alginate beads (PDAB); effects of variables such as solution agitation, solution pH, temperature, and experimental time; and to determine kinetic process models, maximum biopolymer adsorption, and the activation energy of the process.

2. Materials and methods

2.1. Chemical reagents

All reagents used were analytical grade. All solutions were prepared using deionized water. Cobalt solutions were prepared from $CoSO_4 \cdot 7H_2O$ and alginate beads were prepared from low viscosity alginic acid sodium salt from brown algae (Sigma–Aldrich).

2.2. Preparation of barium alginate beads

Protocols following Ibáñez and Umetsu (Ibáñez and Umetsu, 2002) were used in the production of the protonated dry alginate beads. These alginate beads have alginic acid chains which are intertwined with Ba to generate PDAB-Ba. The chemical formula for sodium alginate is $(C_6H_7NaO_6)_x$. Briefly, sodium alginate was dissolved in deionized water (2%w/w solution) and a $BaCl_2$ solution was dripped at concentration 50 mmol dm^{-3} with a 0.005 dm^3 syringe to obtain uniform beads. Beads were protonated in a solution of 1 mol dm^{-3} HNO_3 over 12 hours, then rinsed with deionized water several times. Beads were then subjected to a drying stage at room temperature (298 ± 0.1K). Alginate bead diameters obtained were 1.0 ± 0.1 mm.

2.3. Experimental procedure

Experiments were performed with magnetic stirrer. In typical procedure, 80 mg of alginate beads were added to 0.4 dm^3 cobalt solution with known concentration, and experimental conditions were varied depending on the experiment. The pH was adjusted with 0.05 mol dm^{-3} NaOH for 360 minutes at 293 K. After agitation, beads were removed, and solution samples were obtained to determine Co(II) concentration. Recovery experiments were performed in triplicate, and average values are reported.

2.4. Analytic methodology

Cobalt concentration was determined by means of an inductively coupled plasma atomic emission spectrometer (ICP/AES) (M Series, Thermo, Electron Corporation). The recovery of cobalt (q_t, ×10^{-3} kg kg^{-1} of PDAB) using alginate beads was determined by the following equation:

$$q_t = \frac{(C_0 - C_t)}{m} \cdot V \tag{1}$$

where C_0 and C_t (×10^{-6} kg dm^{-3}) are initial concentration of C_0 at time 0 and at time t in the aqueous solution, respectively; V is solution volume (dm^3); and m is dry mass of alginate beads (kg).

Co(II) recovery efficiency (percentage) was calculated using the following equation:

$$R = \frac{(C_0 - C_t)}{C_0} \cdot 100 \tag{2}$$

2.5. Characterization of alginate beads

Alginate beads were characterized by scanning electron microscope (SEM) Tescan Vega LDH and energy-dispersive X-ray spectroscopy (EDS) a Bruker Quantax system with XFlas 4010 detectors. For

the observation and analysis of alginate bead samples, they were cut with gold and graphite, respectively.

3. Results and discussion

3.1. Effects from agitation

Tests were performed with an initial cobalt concentration of 22×10^{-6} kg dm^{-3} at agitation rates between 100 and 500 rev min^{-1} for 360 minutes at temperature 293K. Results obtained without agitation were also incorporated. The main results are presented in Fig. 1, where equilibrium in residual cobalt concentration (10.3×10^{-6} kg dm^{-3}) was reached at 200 rev min^{-1}. This experimental result is equivalent to Co^{2+} recovery of 58.5 kg kg^{-1} of PDAB. At zero stirring speed, a residual concentration of 21.10×10^{-6} kg dm^{-3} is present, which represents Co^{2+} recovery equal to 4.50×10^{-3} kg kg^{-1} of PDAB.

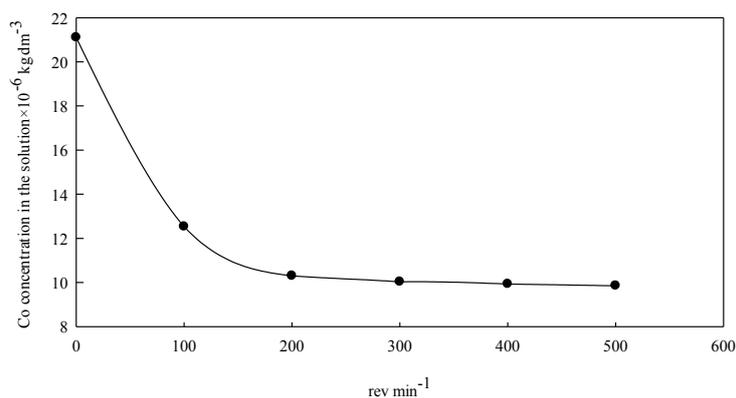

Fig. 1. Residual cobalt concentration as a function of stirring speed (rev min^{-1})

The recovery process has been shown to be independent of mass transfer after about 200 rev min^{-1}. An agitation intensity of 400 rev min^{-1} was chosen for the following experiments.

3.2. Effect of solution pH

Fig. 2 shows the experimental results for the effect of pH on cobalt recovery over 360 minutes. Fig. 2-A shows no variation in cobalt concentration for a pH value equal to 1, from which cobalt ions in solution begin to decrease towards an asymptotic value at pH 6.0, yielding 9.88×10^{-6} kg dm^{-3}. It is observed in this figure that no barium was released during the recovery process, which indicates high PDAB chemical stability.

Fig. 2-B shows a continuous increase in cobalt recovery, towards 60.6×10^{-3} kg kg^{-1} of PDAB at pH 6.0. This recovery value remains constant at higher pH. This behavior is consistent with NaOH consumption, presented in mmol and as a function of pH in Fig. 2-C.

The PDAB contain alginic acid chains with functional carboxyl-type groups. Therefore, under highly acidic pH conditions, cobalt recovery is lower (Fig. 2-A and B). However, at low acidity, functional group dissociation promotes cobalt recovery. Fig. 2-B shows maximum recovery at pH 6.0. This coincides with previous studies, where the apparent dissociation constant of alginic acid is 10^{-4} (Fourest and Volesky, 1996). The higher pH value here is due to alginate beads having a rigid structure and a high carboxylic group density compared to free alginic acid.

Fig. 2-C also shows cobalt recovery and the release of carboxyl group protons. These protons were quantified by NaOH consumption. The following is the ion exchange mechanism for Co^{2+} recovery via PDAB.

$$2\{COO\text{-}H\} + Co^{2+} = \{COO\}_2\text{-}Co + 2H^+ \tag{3}$$

Equation (3) represents cobalt ion recovery from solution. There is a molar relationship for the cobalt ions exchanged with protons released during the process. To corroborate equation (3), Fig. 3 clearly shows that molar ratio $d[H^+]/d[Co^{2+}]$, as a function of pH for an experimental time of 360 minutes, has value 2. This result confirms that equation (3) represents the cobalt PDAB reaction mechanism.
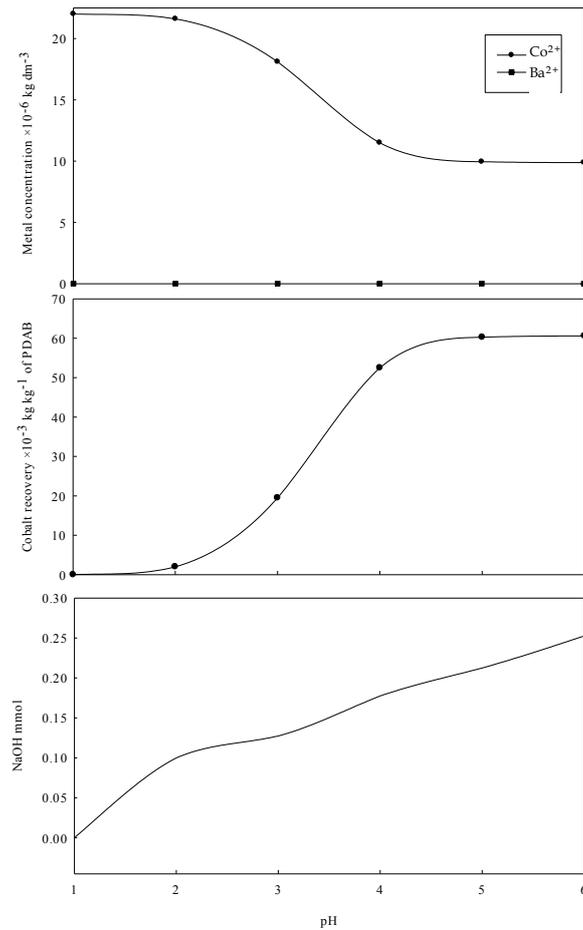
Fig. 2. Experimental results as a function of solution pH. (A) Concentration of Co^{2+} and Ba^{2+} in the solution; (B) recovery of Co^{2+} with PDAB; and (C) NaOH consumption.
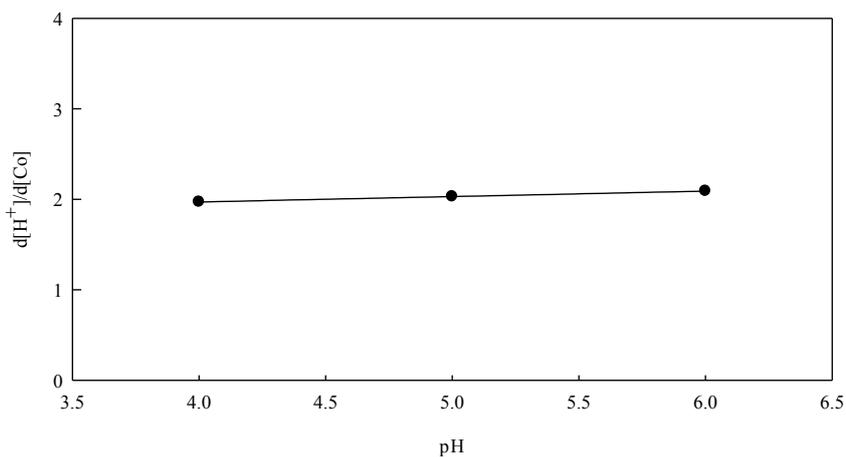

Fig. 3. Variation of $d[H^+]/d[Co^{2+}]$ molar ratio as a function of pH

Experiments showed alginate bead structural changes, i.e., a certain degree of bead swelling. Fig. 4 shows PDAB diameter variation as a function of pH. For pH values less than 2.0, no variation in bead diameter was observed. However, pH 6.0 was associated with a 67.8% increase. During cobalt ion capture processes, cobalt ions enter the PDAB in hydrated form, and thus transport water into the PDAB. Regardless, beads were observed to maintain adequate physical stability. When designing ion exchange columns, this degree of swelling and the consequent porosity generated should be taken into consideration.

1290

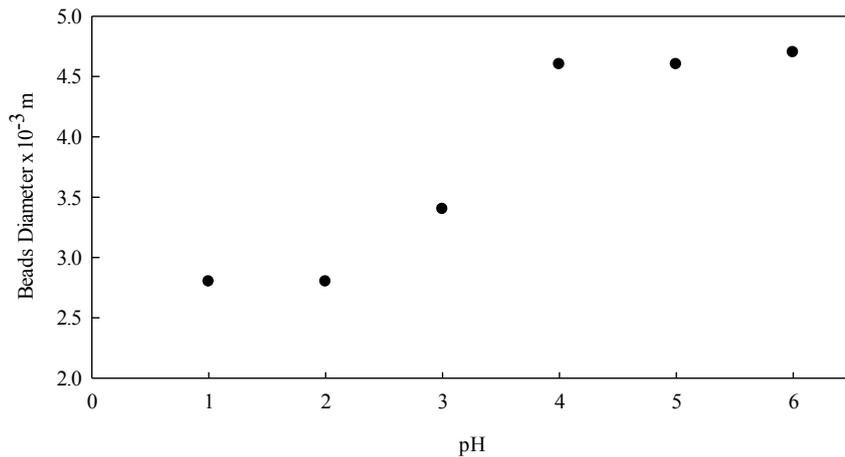Physicochem. Probl. Miner. Process., 55(5), 2019, 1286-1297

Fig. 4. PDAB diameter at the end of each experiment as a function of pH

Cobalt composition across alginate beads was analyzed using backscattered electron imaging (BEI) with an EDS Quantax system for quantification. The average percentage of cobalt through alginate particles is shown by the yellow line in Fig. 5.
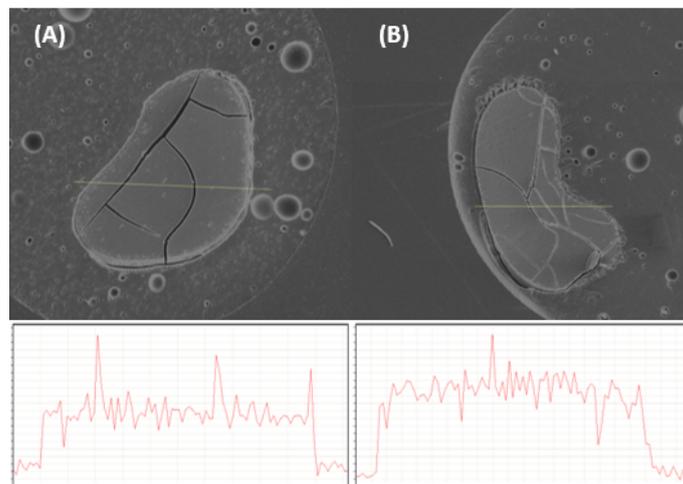

Fig. 5. BEI micrographs of alginates from samples treated at: (A) pH=3.5; and (B) pH=6.0. Cobalt concentration was measured along the thin line

For both figures (5-A and 5-B) the results of the EDS analysis indicated that the distribution of cobalt is uniform throughout the section studied. Fig. 5-A shows that at pH 3.5, average concentration was homogeneously and consistently 3.4%. Fig. 5-B shows that, for pH 6.0, average concentration was 8.70%. These findings corroborate that increased operating pH corresponds to increased average cobalt concentrations inside alginate beads.

3.3. Effect of experimental time

Fig. 6 shows experimental Co^{2+} recovery results over time for initial Co^{2+} concentration of 22 mg dm^{-3}, pH value of 6.0, and 80 mg PDAB. All curves show that the first 120 minutes had sustained increases in Co recovery speed. These decreased until stabilizing at time 300 minutes. Co^{2+} recoveries of 57.6, 81.8, and 105.0×10^{-3} kg kg^{-1} of PDAB were obtained for initial concentrations of 22, 35, and 45×10^{-6} kg dm^{-3}, respectively, at time 360 minutes. These values additionally indicate that increased Co^{2+} concentrations generate increased cobalt recovery.

Solids were analyzed using ESD. Alginate samples were taken at 180 and 360 minutes (initial Co^{2+}=22 mg dm^{-3}). Fig. 7 shows the resulting Co^{2+} distributions for the two alginate bead samples, which indicates that increased cobalt ions in alginate recovery time increases the amount of Co^{2+} throughout

the alginate. Average cobalt concentration in alginate beads was 4.22% Co^{2+} for time 180 minutes, which increased significantly to 8.70% for time 360 minutes. The amount of cobalt in PDAB is here parallel to the behavior observed in Fig. 6. Average cobalt concentration in the beads is also homogeneous in both cases.
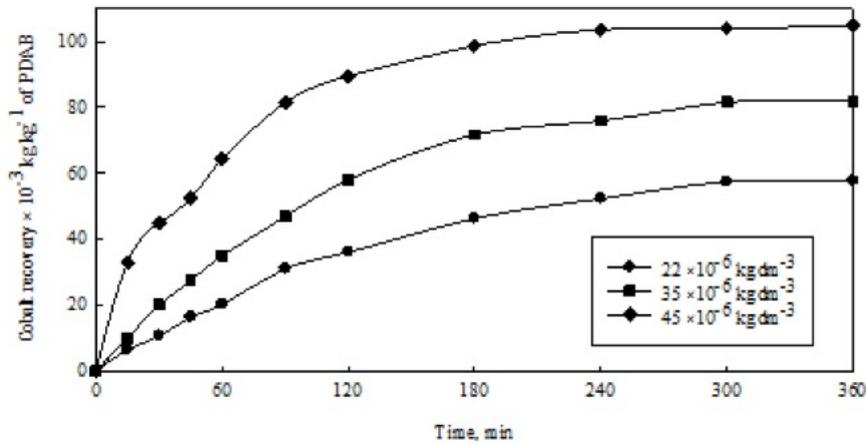

Fig. 6. Co^{2+} recovery at initial concentrations of 22, 35, and 45 mg dm^{-3}; constants were pH 6.0, time 360 minutes, and temperature 293K
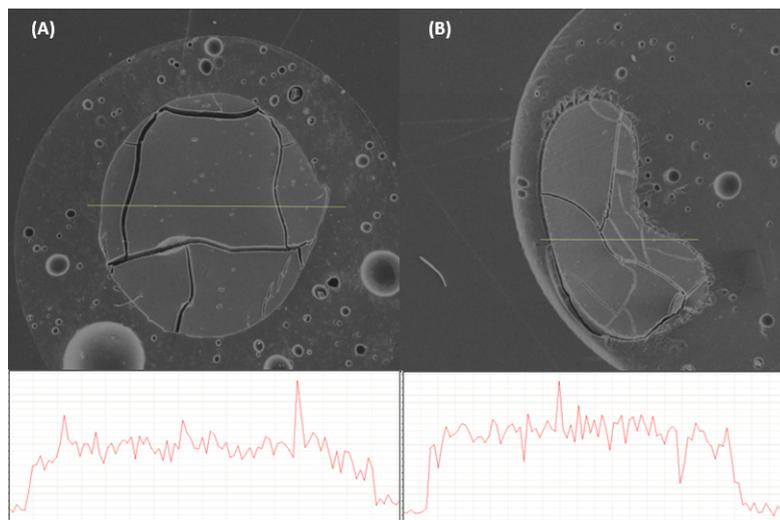

Fig. 7. BEI micrographs of alginates from samples treated for: (A) 180 minutes; and (B) 360 minutes

3.4. Cobalt recovery kinetics

Cobalt recovery kinetics were analyzed using the following models: Lagergren pseudo-first order (4) and pseudo-second order (5); Elovich model (6); Bangham model (7); and intraparticular diffusion (8).

$$\log(q_e - q_t) = \log(q_e) - \left(\frac{k_1}{2.303}\right) \cdot t \qquad (4)$$

$$\frac{t}{q_t} = \frac{1}{k_2 q_e^2} + \frac{1}{q_e} \cdot t \qquad (5)$$

$$q_t = a + b \cdot \ln(t) \qquad (6)$$

$$\log\left(\log\left(\frac{c_0}{c_0 - q_t \cdot m}\right)\right) = \log\left(\frac{k_0 \cdot m}{2.303 \cdot V}\right) + \alpha \cdot \log(t) \qquad (7)$$

$$q_t = k_f \cdot t^{0.5}. \qquad (8)$$

Initial cobalt concentrations were 22, 35, and 45×10^{-6} kg dm^{-3} with 80 mg of PDAB, pH value 6.0, and contact time up to 360 minutes. Experimental data were obtained from Fig. 6. All models were analyzed. The highest correlation was the pseudo-first order Lagergren model, with $R^2 > 0.99$. Fig. 8 (log (q_e-q_t)

versus t) shows the very good linear fit of the experimental data with the line produced by the model. Velocity constants k_1 were obtained from the slopes for the three different initial concentrations of cobalt. Table 1 shows the values of the correlation coefficients for each initial cobalt concentration as well as the velocity constants. This model would indicate that the ion exchange reaction between the cobalt ions and protons (from the alginate) would be carried out by intraparticular diffusion through the beads of alginate.
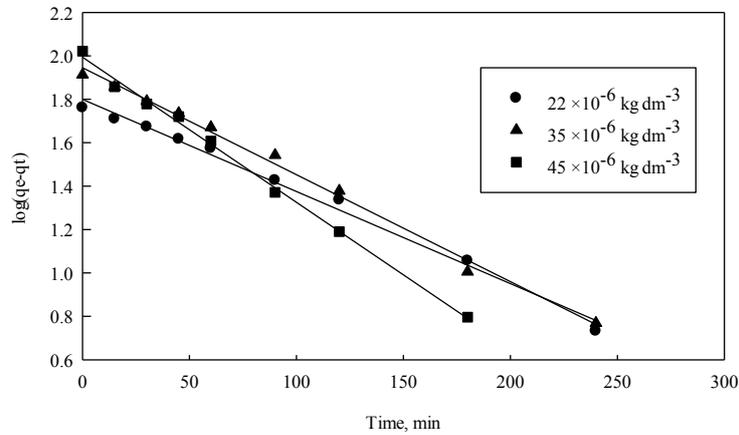

Fig. 8. Linear representation of the pseudo-first order kinetic model for cobalt recovery at 293 K. Initial concentrations of Co^{2+}=22, 35, and 45×10^{-6} kg dm^{-3}

Table 1. Correlation coefficient and velocity constant for applied pseudo first-order model of cobalt recovery with PDAB

Concentration Co(II), kg dm^{-3}	R^2	k_1, min^{-1}
22×10^{-6}	0.991	0.0097
35×10^{-6}	0.993	0.0113
45×10^{-6}	0.997	0.0154

3.5. Isotherm values and models

Fig. 9 shows the experimental results for cobalt ion recovery as a function of equilibrium concentration at pH values of 2.5, 3.5, and 6.0. This figure indicates complete Co-PDAB saturation at equilibrium concentration 500×10^{-6} kg dm^{-3} for all pH values. The isotherm values found were 99.5, 142.5, and 235.0×10^{-3} kg kg^{-1} of PDAB for pH values 2.5, 3.5, and 6.0, respectively.

A high Co^{2+} recovery value, equal to 57.7×10^{-3} kg kg^{-1} of PDAB, was found for very dilute cobalt solutions at pH 6.0. This indicates that even highly dilute conditions will result in important cobalt recovery levels.

The experimental data in Fig. 9 were adjusted to the Langmuir (9), Freundlich (10) and Temkin (11) adsorption isotherm models. The parameters of these models are presented in Table 2. Experimental data was best fit by the Langmuir model (R^2=0.995) for the three pH values. The maximum recovery value given by the model was 263.2, 169.5, and 166.7×10^{-3} kg kg^{-1} of PDAB for pH values 6.0, 3.5, and 2.5, respectively. This model suggests that cobalt molecules are absorbed on the alginate surface, forming a monomolecular layer.

$$\frac{C_e}{q} = \frac{1}{b \cdot q_e} + \frac{C_e}{q_e} \tag{9}$$

$$Log(q) = Log(a) + \frac{1}{n} \cdot Log(C_e) \tag{10}$$

$$q = B \cdot Ln(A_T) + B \cdot Ln(C_e) \tag{11}$$

3.6. Effect of temperature

The effect of temperature (283 to 333K) was studied for an initial concentration of 22×10^{-6} kg dm^{-3} and pH 6.0. As the temperature increased, so did Co^{2+} recovery. At 283K, cobalt recovery reached

17.75×10^{-3} kg kg^{-1} of PDAB at time 90 minutes; at temperature 313K, recovery was 38.13×10^{-3} kg kg^{-1} of PDAB for the same experimental time: in short, Co^{2+} recovery was doubled by an increase of 30 degrees.
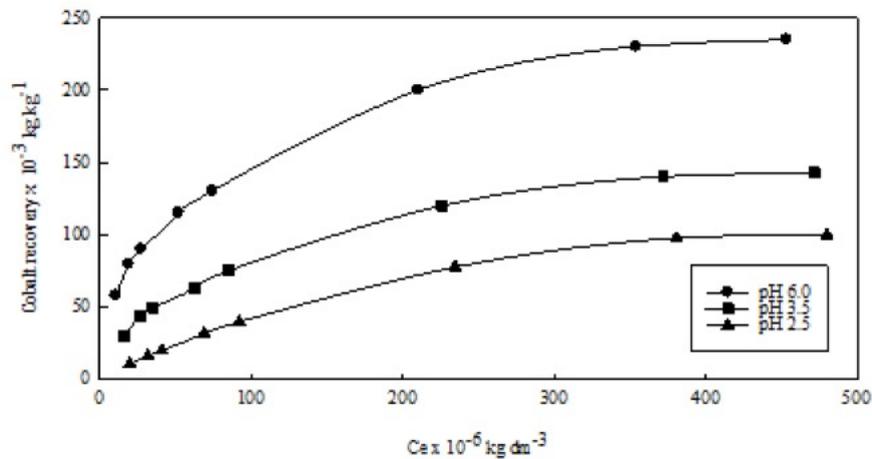

Fig. 9. Cobalt recovery as a function of equilibrium concentration for different pH values

Table 2. Parameters of the Langmuir, Freundlich, and Temkin adsorption models and correlation coefficients (R^2)

pH	Langmuir			Freundlich			Temkin		
	q_{max}	b	R^2	k	n	R^2	a	b	R^2
2.5	166.7	0.003	0.990	1.4	1.389	0.986	0.051	30.704	0.972
3.5	169.5	0.011	0.995	9.4	2.189	0.987	0.121	35.362	0.984
6.0	263.2	0.018	0.994	25.8	2.684	0.992	0.243	49.784	0.984

q_{max} - Langmuir maximum uptake, b - Langmuir isotherm parameter, k, n - Freundlich isotherm constants, a, b - Temkin isotherm constants
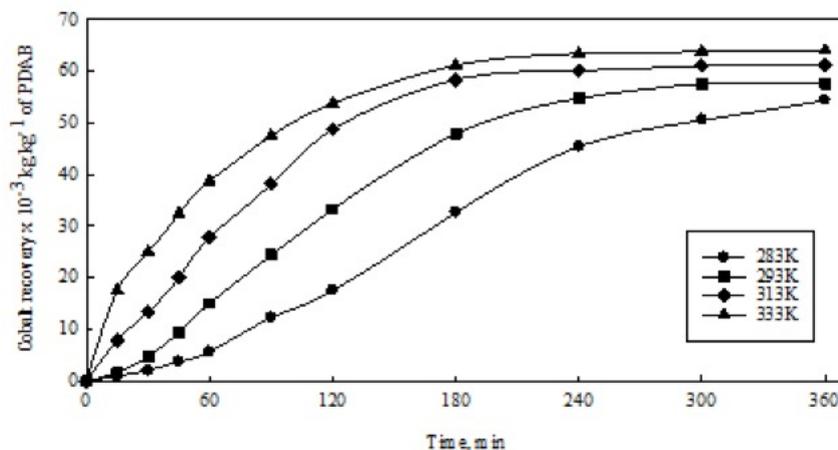

Fig. 10. Effect of temperature on cobalt ion recovery at initial concentration 22×10^{-6} kg dm^{-3} and pH 6.0

Alginate beads were analyzed be ESD. Solid samples were obtained at temperatures 283 and 293K. Fig. 11 shows these measurements, where it can be seen that cobalt concentration in alginate beads remains stable for both temperatures; and that increased temperatures have higher cobalt concentrations in alginate, corroborating data in Fig. 10. The EDS data showed that average percentage of cobalt in beads at temperatures 283 and 293K were 5.03 and 8.69%, respectively. This confirms recovery process behavior of increased temperature resulting in increased Co^{2+} recovery.

Since the pseudo-first order Lagergren velocity model fit experimental data very well, this model was used to adjust temperature-related experimental data (Fig. 10) to obtain kinetic constants (k_1). Fig. 12 shows a log plot (q_e-q_t) of experimental data obtained in Fig. 10 as a function of time for the 283 to 333K temperature range. A good linear fit for kinetic data is shown, with regression coefficients (R^2)

equal to 0.99 for the entire temperature range, demonstrating the applicability of equation (4). The kinetic constant values for the temperature range studied were obtained from the slopes of the straight lines and are listed in Table 3.
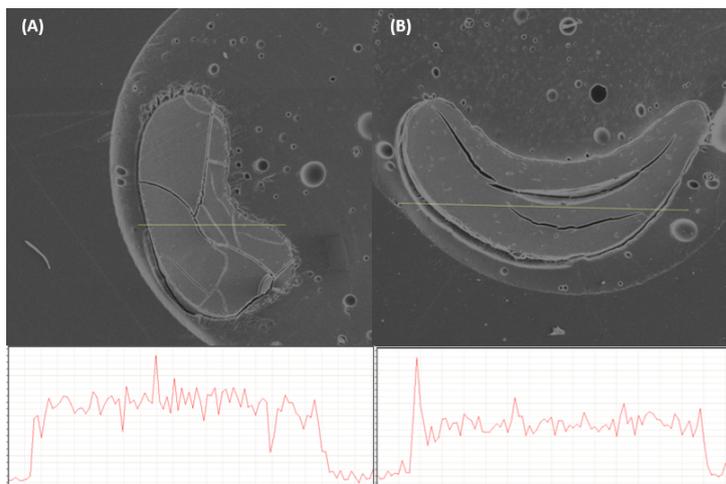

Fig. 11. Scanning electron microscope images of alginate samples treated at: (A) 293K; and (B) 283K
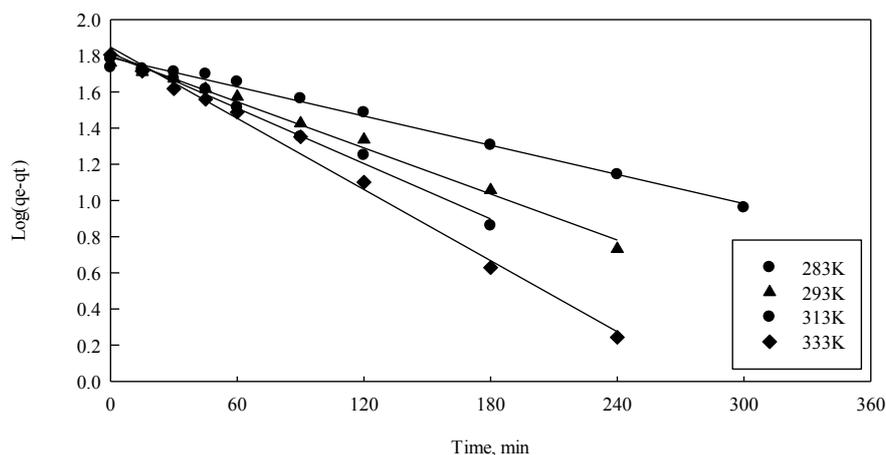

Fig. 12. Co^{2+} recovery kinetics from PDAB for temperatures of 283, 293, 313, and 333K

Table 3. Calculated data for activation energy

T [K]	1000/T (1/K)	k_1	$-\ln k_1$
283	3.5336	0.006	5.083
293	3.4129	0.010	4.638
313	3.1949	0.012	4.448
333	3.0030	0.015	4.186

Calculated kinetic constant values (k_1) were used to generate the Arrhenius graph in Fig. 13, which shows a good linear fit ($R^2=0.92$) of the kinetic constants. The calculated activation energy was 12.8 kJ mol^{-1} for temperature range 283 to 333K. This activation energy value is typical for kinetic diffusion models.

3.7. Elution of Co^{2+} from PDAB

Experiments conducted to preliminarily evaluate the Co^{2+} elution process from PDAB evaluated sulfuric acid (H_2SO_4) concentrations of 0.024×10^{-3}, 0.08×10^{-3}, and 0.72×10^{-3} kg dm^{-3}. Cobalt-laden PDAB samples were obtained from previous experiments. The results in Fig. 14 show that increased acid concentrations yield increased Co^{2+} elution percentages of 44.5, 77.4, and 98.2%, respectively. Visually,

it was observed that the alginate beads remained intact; that is, they did not suffer physical alterations. These results indicate that protonated dry alginate beads can be reused in recovering cobalt ions.
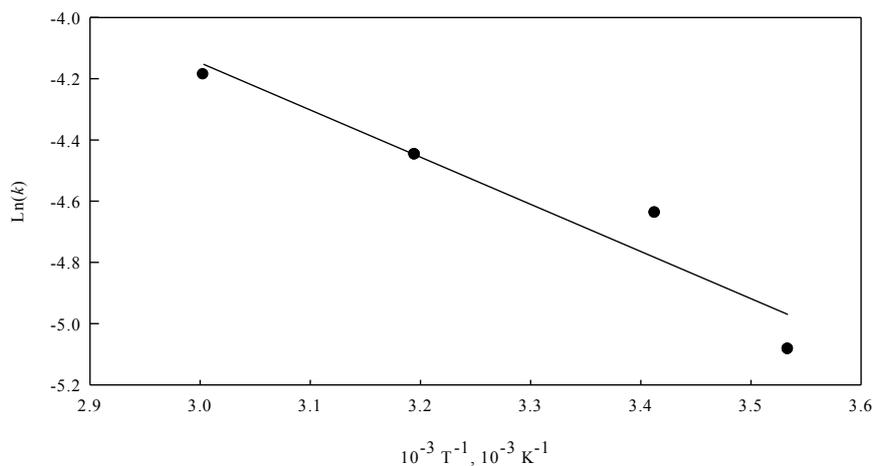

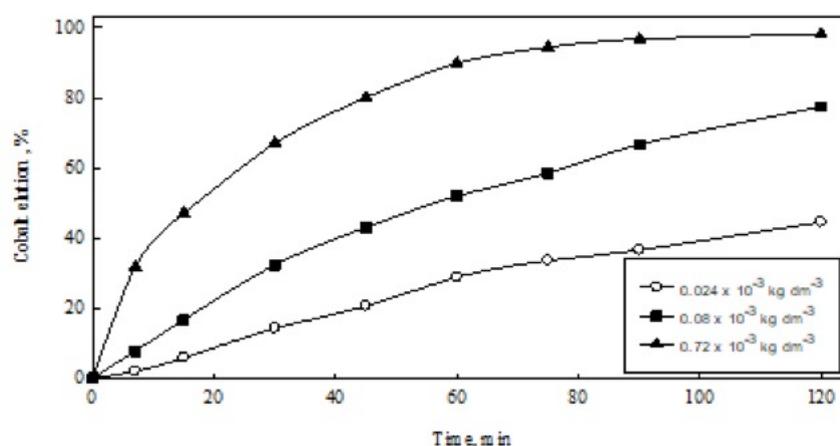Fig. 13. Arrhenius graph for cobalt ion recovery from PDAB

Fig. 14. Elution of Co^{2+} from PDAB with sulfuric acid concentrations of 0.024×10^{-3}, 0.08×10^{-3}, 0.72×10^{-3} kg dm^{-3}

3.8. Comparison with other biosorbents

Results from other cobalt recovery techniques using other biosorbent materials are shown in Table 4, a summary of work carried out since 2000. Recovery of Co^{2+} with PDAB is included for comparison. The table clearly shows that cobalt recovery in this research is significantly higher than other biosorbent

Table 4. Cobalt recovery with different biosorbents

Sorbent material	Recovery, mg/g	pH	Reference
Activates carbon of potato waste	373	8.0	(Kyzas et al., 2016)
AMP-PAN	9.4	5.0	(Park et al., 2010)
Clinoptilolite	2.9	5.0	(Smičiklas et al., 2007)
11 A tobermorite	10.5	-	(Coleman et al., 2006)
Magnetite	0.25	7.0	(Ebner et al., 2001)
Banana pseudostem	33	6.0	(Rodrigues et al., 2013)
Silica gel	109.02	5.5	(Arakaki et al., 2013)
Palygorskite	74.84	-	(Oliveira et al., 2013)
Chitosan	67.18	5.5	(Monier et al., 2010)
Celam biopolymer	5.72	6	(Silva Filho et al., 2013)
Protonated dry alginate beads	235	6	This work

techniques analyzed. The closest competitor seems to be recovery with activated potato-waste biosorbent carbon. Further economic analysis is needed to compare these techniques.

4.   Conclusions

In sum, solution pH was the most preponderant factor, with pH 6.0 yielding highest Co^{2+} recovery, reaching a value of 60.6×10^{-3} kg kg^{-1} of PDAB using only 80 mg of PDAB. Increased agitation during the process also increased cobalt recovery. The cobalt recovery mechanism is given by the ion exchange with the protons released from the carboxylic group of the alginate.

The Langmuir adsorption model fit experimental data very well, suggesting maximum Co^{2+} recovery at 235×10^{-3} kg kg^{-1} of PDAB (pH = 6.0). The latter value is high for most sorbents described for cobalt recovery in the literature. This recovery was represented by the pseudo-first order kinetic equation with a velocity constant of 0.0097 min^{-1}. Temperature played an important role, with a 30K increase doubling cobalt recovery. The calculated activation energy was 12.8 kJ mol^{-1} for temperature range 283 to 333K.

Finally, it was possible to elute cobalt from saturated PDAB, with preliminary experiments showing concentrations of 0.72×10^{-3} kg dm^{-3} of H_2SO_4 yielding 98.2% elution. The PDAB is one of the biosorbents with the highest recovery of cobalt in the area registered since 2000, indicating its potential use in the industry.

References

ARACENA, A., GUAJARDO, N., IBÁÑEZ, J.P., JEREZ, O., CARLESI, C., 2015. *Uptake of nickel ions from aqueous solutions using protonated dry alginate beads*. Can. Metall. Q. 54, 58–65.

ARACENA, A., ÁLVAREZ, C., JEREZ, O., GUAJARDO, N., 2019. *Uptake of copper ion using protonated dry alginate beads from dilute aqueous solutions*. Physicochem. Probl. Miner. Process. 55, 732-744.

ARAKAKI, L.N.H., FILHA, V.L.S.A., GERMANO, A.F.S., SANTOS, S.S.G., FONSECA, M.G., SOUSA, K.S., ESPÍNOLA, J.G.P., ARAKAKI, T., 2013. *Silica gel modified with ethylenediamine and succinic acid-adsorption and calorimetry of cations in aqueous solution.* Thermochim. Acta 556, 34–40.

COLEMAN, N.J., BRASSINGTON, D.S., RAZA, A., MENDHAM, A.P., 2006. *Sorption of Co2+ and Sr2+ by waste-derived 11 Å tobermorite*. Waste Manag. 26, 260–267.

EBNER, A.D., RITTER, J.A., NAVRATIL, J.D., 2001. *Adsorption of Cesium, Strontium, and Cobalt Ions on Magnetite and a Magnetite−Silica Composite*. Ind. Eng. Chem. Res. 40, 1615–1623.

FENG, D., ALDRICH, C., TAN, H., 2000. *Treatment of acid mine water by use of heavy metal precipitation and ion exchange*. Miner. Eng. 13, 623–642.

FOUREST, E., VOLESKY, B., 1996. *Contribution of Sulfonate Groups and Alginate to Heavy Metal Biosorption by the Dry Biomass of Sargassum fluitans.* Environ. Sci. Technol. 30, 277–282.

GÜLER, E., SEYRANKAYA, A., 2016. *Precipitation of impurity ions from zinc leach solutions with high iron contents - A special emphasis on cobalt precipitation*. Hydrometallurgy 164, 118–124.

HACHEMAOUI, A., BELHAMEL, K., 2017. *Simultaneous extraction and separation of cobalt and nickel from chloride solution through emulsion liquid membrane using Cyanex 301 as extractant*. Int. J. Miner. Process. 161, 7–12.

HO, Y.S., MCKAY, G., 2000. *The kinetics of sorption of divalent metal ions onto sphagnum moss peat*. Water Res. 34, 735–742.

HUANG, J.D., TAN, M.X., XU, J.L., LUO, J.Z., LIU, J.Z., ZHANG, R.Z., LIU, J., 2019. *Gel-assisted synthesis of Cu-Co-S nanosheets forlithium-ion batteries.* Applied Surface Science 488, 537-545

IBÁÑEZ, J.P., ARACENA, A., 2014. *Uptake of Zn2+ from dilute aqueous solutions using protonated dry alginate beads*. Can. Metall. Q. 53, 82–87.

IBÁÑEZ, J.P., UMETSU, Y., 2004. *Uptake of trivalent chromium from aqueous solutions using protonated dry alginate beads*. Hydrometallurgy 72, 327–334.

IBÁÑEZ, J.P., UMETSU, Y., 2002. *Potential of protonated alginate beads for heavy metals uptake*. Hydrometallurgy 64, 89–99.

IBÁÑEZ, J.P., UMETSU, U., 2008. *Uptake of cd2+ from Aqueous Solutions Using Protonated Dry Alginate Beads.* Can. Metall. Q. 47, 45–50.

JIANG, J.L., MA, C., MA, T.F., ZHU, J.J., LIU, J.H., YANG, G., YANG, Y., 2019. *A novel CoO hierarchical morphologies on carbon nanofiber for improved reversibility as binder-free anodes in lithium/sodium ion batteries.* Journal of Alloys and Compounds 794, 385-395.

KYZAS, G.Z., DELIYANNI, E.A., MATIS, K.A., 2016. *Activated carbons produced by pyrolysis of waste potato peels: Cobalt ions removal by adsorption. Colloids Surfaces A Physicochem.* Eng. Asp. 490, 74–83.

LEYSSENS, L., VINCK, B., VAN DER STRAETEN, C., WUYTS, F., MAES, L., 2017. *Cobalt toxicity in humans — A review of the potential sources and systemic health effects.* Toxicology 387, 43–56. https://doi.org/10.1016/J.TOX.2017.05.015

MONIER, M., AYAD, D.M., WEI, Y., SARHAN, A.A., 2010. *Adsorption of Cu(II), Co(II), and Ni(II) ions by modified magnetic chitosan chelating resin.* J. Hazard. Mater. 177, 962–970.

OLIVEIRA, A.M.B.M., COELHO, L.F.O., GOMES, S.S.S., COSTA, I.F., FONSECA, M.G., DE SOUSA, K.S., ESPÍNOLA, J.G.P., DA SILVA FILHO, E.C., 2013. *Brazilian Palygorskite as Adsorbent for Metal Ions from Aqueous Solution — Kinetic and Equilibrium Studies.* Water, Air, Soil Pollut. 224, 1687.

PARK, Y., LEE, Y.-C., SHIN, W.S., CHOI, S.-J., 2010. *Removal of cobalt, strontium and cesium from radioactive laundry wastewater by ammonium molybdophosphate–polyacrylonitrile (AMP–PAN).* Chem. Eng. J. 162, 685–695.

QUI, S.H., WU, D.X., DONG, Y., LIAO, J.Q. FOSTER, C.W., O'DWYER, C., FENG, Y.Z., LIU, C.T., MA, J.M., 2019. *Cobalt-based electrode materials for sodium-ion batteries.* Chemical Engineering Journal 370, 185-207.

RODRIGUES, N.F.M., SANTANA, S.A.A., BEZERRA, C.W.B., SILVA, H.A.S., MELO, J.C.P., VIEIRA, A.P., AIROLDI, C., SILVA FILHO, E.C., 2013. *New Chemical Organic Anhydride Immobilization Process Used on Banana Pseudostems: A Biopolymer for Cation Removal.* Ind. Eng. Chem. Res. 52, 11007–11015.

SILVA FILHO, E.C., SANTOS JÚNIOR, L.S., SILVA, M.M.F., FONSECA, M.G., SANTANA, S.A.A., AIROLDI, C., 2013. *Surface cellulose modification with 2-aminomethylpyridine for copper, cobalt, nickel and zinc removal from aqueous solution.* Mater. Res.

SMIČIKLAS, I., DIMOVIĆ, S., PLEĆAŠ, I., 2007. *Removal of Cs1+, Sr2+ and Co2+ from aqueous solutions by adsorption on natural clinoptilolite.* Appl. Clay Sci. 35, 139–144.

SÜRÜCÜ, A., EYÜPOGLU, V., TUTKUN, O., 2010. *Selective separation of cobalt and nickel by supported liquid membranes.* Desalination 250, 1155–1156.

WANG, G.X., CHEN, Y., KONSTANTINOV, K., LINDSAY, M., LIU, H.K., DOU, S.X., 2002. *Investigation of cobalt oxides as anode materials for Li-ion batteries.* Journal of Power Sources 109, 142-147